Improved leakage and ferroelectric properties of Mn and Ti codoped BiFeO3 thin films

doi: 10.1063/1.3098408

Improved leakage and ferroelectric properties of Mn and Ti codoped $BiFeO_3$ thin films

T. Kawae,[a] Y. Terauchi, H. Tsuda, M. Kumeda, and A. Morimoto
Graduate School of Natural Science and Technology, Kanazawa University, Kakuma-machi, Kanazawa, Ishikawa 920-1192, Japan

(Received 27 January 2009; accepted 20 February 2009; published online 18 March 2009)

Polycrystalline $BiFeO_3$ (BFO), Ti-doped BFO, Mn-doped BFO, and (Mn, Ti)-codoped BFO (BFMT) thin films were fabricated on $Pt/SrTiO_3$ (100) substrate by pulsed laser deposition. Observed leakage current behavior in those ion-doped BFO films indicated the dominance of space-charge-limited current in the high electric field region. The leakage current of the BFMT film was much reduced in relation to the other films due to the formation of deep traps. In the BFMT film, well saturated *P-E* hysteresis curves were observed. Remanent polarization and coercive field for maximum electric field of 2100 kV/cm were 75 $\mu C/cm^2$ and 310 kV/cm, respectively. © *2009 American Institute of Physics*. [DOI: 10.1063/1.3098408]

Excellent ferro-/piezoelectric properties have been reported in the $BiFeO_3$ (BFO) thin films comparable to those of $Pb(Zr_xTi_{1-x})O_3$,[1–3] and thus the BFO is expected as an alternative Pb-free ferro-/piezoelectric material. However, the large leakage current of BFO thin films at room temperature (RT) is known to be a serious problem, which could limit the various applications of this material.

In the past several years, site-engineering technique by substitution of small amount of impurities was proposed to solve this problem, and reduced leakage current properties were reported.[4–11,15] The site-engineering technique is quite important from industrial aspects because this technique can be applied to most deposition methods. However, it is not easy to reduce the leakage current of BFO films by a single ion-doping method since the excess substitution causes an increase in leakage current in the films.[6,7] Besides, modification of electrical properties of BFO films by ion doping at Bi site is quite difficult because of the degradations in ferroelectric properties, although rare-earth elements doped at Bi site is effective to reduce the impurity phases due to bismuth and oxygen vacancies.[5,8,9] Therefore, we propose a new combination of Mn and Ti as codoping elements for Fe site of BFO thin films. In this work, we report the synthesis and characterization of (Mn, Ti)-codoped BFO (BFMT) thin films by comparing with those of pure BFO, Ti-doped BFO (BFT), and Mn-doped BFO (BFM) thin films. Moreover, it is required to reduce the leakage current of BFO films in the high electric field region (at least more than 400 kV/cm) since coercive electric fields of BFO film capacitors are generally 300–500 kV/cm. Hence, we also discuss the change in conduction mechanism in the high electric field region by ion doping in the BFO thin films.

BFO, BFT, BFM, and BFMT thin films were deposited on Pt-coated (100) $SrTiO_3$ (STO) substrates with thicknesses ranging from 220 to 240 nm, using a conventional pulsed laser deposition (PLD) system. The ceramic targets with metal compositions of $Bi_{1.1}FeO_3$, $Bi(Fe_{0.98}Ti_{0.02})O_3$, $Bi_{1.1}(Fe_{0.97}Mn_{0.03})O_3$, and $Bi(Fe_{0.95}Mn_{0.03}Ti_{0.02})O_3$ were used for deposition of BFO, BFT, BFM, and BNFM films, respectively. The details of thin film fabrication were described in the previous work.[4] To investigate the electrical properties of films, Au top electrodes were deposited by thermal evaporation on the film, resulting in metal-insulator-metal (MIM) capacitors. The surface morphologies of the films were studied using an atomic force microscope (AFM) (Autoprobe-cp, Park Scientific Instruments). The crystal structure of the films was determined by x-ray diffraction (XRD) with Cu $K\alpha$ radiation. The polarization and leakage current properties of MIM capacitors were characterized using FCE-1A (Toyo) and RT-66A (Radiant Technology) test systems. All measurements were performed at RT.

Figure 1(a) shows the AFM images of the films. The grain size of BFM film becomes larger and the film surface becomes denser than that in the BFO film. Although the detailed growth mechanism is not clear yet, similar enhanced grain growth and improved surface morphology in Mn-doped BFO films have been observed.[6] In the case of BFT film, the grain size was reduced to 100–300 nm in size, and the surface morphology was changed to dense and uniform compared with other specimens. As a result, the surface roughness (R_{rms}) was remarkably improved. Similar tendencies have been observed in the BFO films doped with rare-earth elements due to the increase in crystallization temperature.[4,7,8,11] Thus, this behavior seems to be mainly caused by a rise in crystallization temperature due to the chemical bond strength of Ti–O since the melting tempera-

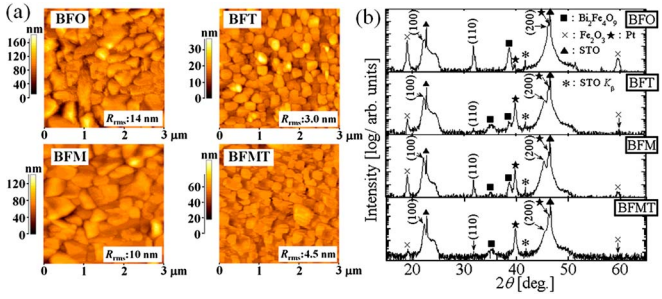

FIG. 1. (Color online) (a) AFM images and (b) XRD patterns for fabricated films grown on Pt-coated (100) STO substrate. The root mean square values of surface roughness of films are shown in the inset of AFM images. Symbols in XRD patterns indicate the impurity phases and substrate.

[a]Author to whom correspondence should be addressed. Electronic mail: kawae@ec.t.kanazawa-u.ac.jp.

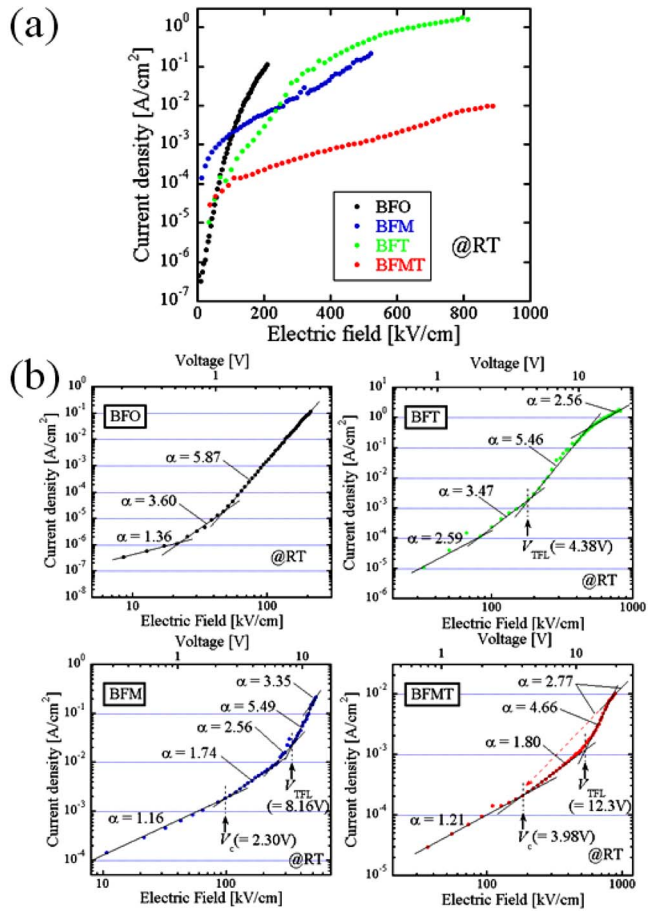

FIG. 2. (Color online) (a) *J-E* curves for fabricated film capacitors at RT. (b) Logarithmic plots of dependence of J as a function of E and V.

ture of TiO_2 (1750 °C) is higher than that of Fe_2O_3 (1570 °C). In the BFMT film, the grain size was widely distributed compared with the BFM and BFT films. Especially, small grains with several tens of nanometers were densely packed in porous parts of the film, and then the quite smooth surface morphology was obtained. Hence, it is suggested that both of the features in BFT and BFM films are transferred to the BFMT film, and the reduction in surface roughness is realized in the film.

Figure 1(b) shows the XRD patterns of the films. All films were found to be polycrystalline BFO with (100) and (110) orientations, although weak peaks of impurity phases ($Bi_2Fe_4O_9$ and Fe_2O_3) due to Bi deficiency were detected. On the other hand, the peak intensities of such impurity phases were smaller in the BFT and BFMT films than those of the BFO and BFM films. This result can be ascribed to the fact that Bi deficiencies during migration of ablated species on the substrate before crystallization were suppressed due to the increase in the crystallization temperature in the BFO by Ti doping, as described in the AFM results. Thus, Ti doping is effective to obtain the BFO single phase in the film.

Figure 2(a) shows the leakage current density versus electric field (*J-E*) properties of fabricated film capacitors. The BFO and BFT films show low leakage current in the low electric field region (<100 kV/cm). However, the leakage current increases rapidly with an increase in the applied electric field. In the BFM film, although the leakage current density is high up to 100 kV/cm compared with other films, the leakage current remains in the order of 10^{-2} A/cm^2 even at 400 kV/cm, as shown in the figure. On the other hand, the BFMT film shows a greatly reduced leakage current compared with other films in a wide range of electric field (60–900 kV/cm).

In order to find out the origin of reduced leakage current in the BFMT film, we discussed the conduction mechanism of fabricated specimens. Figure 2(b) shows the logarithmic plots of dependence of J as a function of E and V for fabricated specimens. As can be seen from the figure, the curves of ion-doped BFO films can be modeled in terms of space-charge-limited current (SCLC).[12,13] In the low field region, the curves follow Ohmic conduction properties ($J \propto E^{\alpha}$: $\alpha \sim 1$). With increasing electric field, the curves change according to the modified Child's law ($J \propto E^{\alpha}$: $\alpha > 1$) conduction, and an abrupt increase in slope in the double logarithm plot occurs since deep traps were completely filled up called as the trap-filled-limit (TFL) region. Finally, at the highest electric field region, the curves reach values according to Child's law conduction ($J \propto E^{\alpha}$: $\alpha \sim 2$). On the other hand, in the case of the BFO film, explicit Child's law region with a slope of ~2 and transition voltages were not observed because the transition voltage might be higher or the leakage conduction might include other mechanisms such as Schottky or Poole–Frenkel conduction.[14] According to Lampert's[12] theory of the SCLC conductions, the transition voltage V_c (Ohmic to modified Child's law) and V_{TFL} (modified Child's law to TFL) are given by the following equations:

$$V_c = \frac{end^2}{2\varepsilon_r \varepsilon_0 \theta}, \tag{1}$$

$$V_{\mathrm{TFL}} = \frac{eN_t d^2}{2\varepsilon_r \varepsilon_0}, \tag{2}$$

where n is the density of electrons in the conduction band, d is the film thickness, ε_r is the static dielectric constant, ε_0 is the permittivity of free space, and N_t is the total trap density. θ represents the ratio of the free carrier density to the density of the filled trapping sites given by

$$\theta = \frac{N_c}{N_t} \exp\left(\frac{-E_t}{k_B T}\right), \tag{3}$$

where N_c is the effective density of states in the conduction band, E_t is the energy level of carrier trap sites, and $k_B T$ is the thermal energy. Then, the leakage current for modified Child's law conduction is determined as

$$J = \frac{9\varepsilon_r \varepsilon_0 \mu \theta E^2}{8d}, \tag{4}$$

where E is the applied electric field and μ is the carrier mobility. Here, V_{TFL} for each specimen was found out as $V_{\mathrm{TFL}}(\mathrm{BFMT}) > V_{\mathrm{TFL}}(\mathrm{BFM}) > V_{\mathrm{TFL}}(\mathrm{BFT})$ from the experimental results in Fig. 2(b), and this indicates that doped ions in the films mainly act as carrier trap sites. Also, V_c for the BFM and BFMT films are much higher than that in the BFT film, which is probably lower than 0.5 V, and the difference of V_{TFL} values among the BFT, BFM, and BFMT films is not so large compared with those of V_c. This suggests that Mn ions give rise to deeper traps than Ti ions do. Thus, it means that deep traps were formed by Mn doping. Moreover, we consider that greatly reduced leakage current of BFMT film

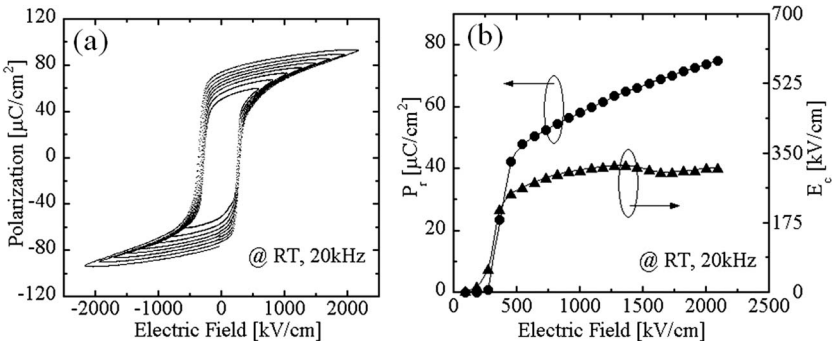

FIG. 3. Ferroelectric properties of BFMT film capacitor measured at RT with measurement frequency of 20 kHz. (a) *P-E* hysteresis loops as a function of electric field. (b) Electric field dependences of remanent polarization and coercive field.

is closely related to such deep trap levels formed by ion doping. Higuchi *et al.*[15] reported the valence state of Mn ions for the Mn-doped BFO-$BaTiO_3$ ceramics from soft x-ray absorption spectroscopy, and Mn ions in that system are located at Fe sites as Mn^{2+} due to the existence of Ti. Then, we deduce that the valence state of Mn ions in the BFMT film is similarly fixed to Mn^{2+} by (Mn, Ti) codoping, and they form trap levels deeper than that of the BFM film. As a result, leakage current of BFMT film in the modified Child's law conduction region has been suppressed compared with the BFM film. The increase in leakage current by excess Mn doping in the BFO films was also observed in our specimens (not shown) same as other groups reported.[6] According to the above speculations, this might be caused by the formation of shallow states because of valence fluctuations of Mn ions. In addition, concerning the suppression of leakage current of BFMT film in low electric field region, it seems that there is the contribution of improvement of surface roughness to some extent. Hence, we consider that the origin of reduced leakage current in the BFMT film in a wide range of electric field is the "formation of deep traps" and "smooth surface morphology" by the synergetic effect due to (Mn, Ti) codoping.

Figure 3(a) shows the polarization versus electric field (*P-E*) curves of BFMT film capacitor. In the other specimens, stable *P-E* curves could not be observed at RT because of its huge leakage current. As shown in the figure, well saturated hysteresis loops were observed with applied electric fields up to 2100 kV/cm. In general, it is not easy to measure the stable *P-E* curves of the BFO films in the high electric field region (>1000 kV/cm) because of the poor breakdown properties. Therefore, the observed result means that both resistor components and breakdown properties in the film were significantly improved. Figure 3(b) shows the electric field dependence of remanent polarization P_r and coercive field E_c in the BFMT film capacitor. P_r and E_c at a maximum electric field of 2100 kV/cm were approximately 75 $\mu C/cm^2$ and 310 kV/cm, respectively. Although P_r is still not saturated, E_c tends to saturate at 1250 kV/cm. Since the observed electric field dependences of P_r value are almost comparable with those of polycrystalline pure BFO film capacitors measured by low temperature or high-speed positive-up–negative-down measurements,[10,16] degradations of ferroelectric properties due to ion doping are almost nothing. Hence, it is concluded that (Mn, Ti) codoping in the BFO film is an effective technique leading to the excellent ferroelectric properties at RT without any serious degradations.

In summary, we prepared the (Mn, Ti)-codoped BFO thin films on Pt/STO substrate by PLD method. The AFM micrographs and XRD analysis indicated that both smooth surface morphology and suppression of impurity phases were realized in the BFMT film. The BFMT film showed greatly reduced leakage current compared with that of other specimens in a wide range of electric fields. The well-saturated *P-E* hysteresis curves were observed at RT. P_r and E_c values for maximum electric field of 2100 kV/cm were 75 $\mu C/cm^2$ and 310 kV/cm, respectively.

The authors would like to thank Professor S. Okamura and Dr. T. Nakajima for their fruitful discussions and technical support to measure the ferroelectric properties of specimens using FCE-1 system.

[1] J. Wang, J. B. Neaton, H. Zheng, V. Nagarajan, S. B. Ogale, B. Liu, D. Viehland, V. Vaithyanathan, D. G. Schlom, U. V. Waghmare, N. A. Spaldin, K. M. Rabe, M. Wuttig, and R. Ramesh, Science **299**, 1719 (2003).
[2] A. H. M. Gonzalez, A. Z. Simoes, L. S. Cavalcante, E. Long, J. A. Varela, and C. S. Riccardi, Appl. Phys. Lett. **90**, 052906 (2007).
[3] J. Wang, H. Zheng, Z. Ma, S. Prasertchoug, M. Wuttig, R. Droopad, J. Yu, K. Eisenbeiser, and R. Ramesh, Appl. Phys. Lett. **85**, 2574 (2004).
[4] T. Kawae, H. Tsuda, and A. Morimoto, Appl. Phys. Express **1**, 051601 (2008).
[5] F. Huang, X. Lu, W. Lin, X. Wu, Y. Kan, and J. Zhu, Appl. Phys. Lett. **89**, 242914 (2006).
[6] S. K. Singh, H. Ishiwara, K. Sato, and K. Maruyama, J. Appl. Phys. **102**, 094109 (2007).
[7] G. D. Hu, X. Cheng, W. B. Wu, and C. H. Yang, Appl. Phys. Lett. **91**, 232909 (2007).
[8] A. Z. Simoes, L. S. Cavalcante, C. S. Riccardi, J. A. Varela, and E. Longo, Curr. Appl. Phys. **9**, 520 (2009).
[9] H. Uchida, R. Ueno, H. Funakubo, and S. Koda, J. Appl. Phys. **100**, 014106 (2006).
[10] H. Naganuma, J. Miura, and S. Okamura, Appl. Phys. Lett. **93**, 052901 (2008).
[11] C. C. Lee and J. M. Wu, Electrochem. Solid-State Lett. **10**, G58 (2007).
[12] M. Lampert, Phys. Rev. **103**, 1648 (1956).
[13] A. R. Chaudhuri and S. B. Krupanidhi, J. Appl. Phys. **98**, 094112 (2005).
[14] G. W. Pabst, L. W. Martin, C. Ying-hao, and R. Ramesh, Appl. Phys. Lett. **90**, 072902 (2007).
[15] T. Higuchi, W. Sakamoto, N. Itoh, T. Shimura, T. Hattori, and T. Yogo, Appl. Phys. Express **1**, 011502 (2008).
[16] H. Naganuma, Y. Inoue, and S. Okamura, Appl. Phys. Express **1**, 061601 (2008).